© 2017. Published by The Company of Biologists Ltd | Journal of Experimental Biology (2017) 220, 2354-2363 doi:10.1242/jeb.156125

RESEARCH ARTICLE

Identification of the septate junction protein gliotactin in the mosquito *Aedes aegypti*: evidence for a role in increased paracellular permeability in larvae

Sima Jonusaite*, Scott P. Kelly and Andrew Donini

ABSTRACT

Septate junctions (SJs) regulate paracellular permeability across invertebrate epithelia. However, little is known about the function of SJ proteins in aquatic invertebrates. In this study, a role for the transmembrane SJ protein gliotactin (Gli) in the osmoregulatory strategies of larval mosquito (*Aedes aegypti*) was examined. Differences in *gli* transcript abundance were observed between the midgut, Malpighian tubules, hindgut and anal papillae of *A. aegypti*, which are epithelia that participate in larval mosquito osmoregulation. Western blotting of Gli revealed its presence in monomer, putative dimer and alternatively processed protein forms in different larval mosquito organs. Gli localized to the entire SJ domain between midgut epithelial cells and showed a discontinuous localization along the plasma membranes of epithelial cells of the rectum as well as the syncytial anal papillae epithelium. In the Malpighian tubules, Gli immunolocalization was confined to SJs between the stellate and principal cells. Rearing larvae in 30% seawater caused an increase in Gli protein abundance in the anterior midgut, Malpighian tubules and hindgut. Transcriptional knockdown of *gli* using dsRNA reduced Gli protein abundance in the midgut and increased the flux rate of the paracellular permeability marker, polyethylene glycol (molecular weight 400 Da; PEG-400). Data suggest that in larval *A. aegypti*, Gli participates in the maintenance of salt and water balance and that one role for Gli is to participate in the regulation of paracellular permeability across the midgut of *A. aegypti* in response to changes in environmental salinity.

KEY WORDS: Larval mosquito, Osmoregulation, Midgut permeability, Septate junctions, Gliotactin

INTRODUCTION

Larval mosquitoes occur in a variety of aquatic habitats ranging from man-made containers and ditches to woodland pools and marshes. The salinity of these habitats varies from nearly salt-free freshwater (FW) to brackish water (BW) and seawater. In FW environments, the osmotic gradient between the circulating hemolymph of the larva and the external aquatic medium favors the influx of water into the body and the efflux of ions from the body. Under saline conditions, the osmotic gradient is reversed and the larva is susceptible to passive water loss and excessive salt gain. The survival of mosquito larvae depends on their ability to regulate the influx and efflux of ions and water across osmoregulatory epithelia such as those of the midgut, Malpighian tubules, hindgut and anal papillae (Clements, 1992; Bradley, 1994; Donini and O'Donnell, 2005; Del Duca et al., 2011). Studies examining the role of osmoregulatory epithelia in the maintenance of salt and water balance in larval mosquitoes have generally focused on transcellular mechanisms/routes of ion movement, through which actively driven ion transport takes place (Bradley, 1995; Patrick et al., 2002; Donini et al., 2006, 2007; Smith et al., 2008; Del Duca et al., 2011). In contrast, far less emphasis has been placed on the paracellular pathway which is regulated by the specialized cell–cell junctions known as septate junctions (SJs). As a result, the role of SJs in the maintenance of salt and water balance in mosquito larvae is poorly understood.

In cross-section electron microscopy, SJs display a characteristic ladder-like structure between adjacent cells with septa spanning a 15–20 nm intercellular space (Green and Bergquist, 1982). SJs typically form circumferential belts around the apicolateral regions of epithelial cells and control the movement of biological material through the paracellular route (Jonusaite et al., 2016a). Several morphological variants of SJs exist across invertebrate phyla and some animals possess multiple types of SJs that are specific to different epithelia (Green and Bergquist, 1982; Jonusaite et al., 2016a). Molecular analyses of insect SJs have largely been performed in *Drosophila melanogaster*, where two types of SJs are present: the pleated SJ (pSJ) and the smooth SJ (sSJ), which are found in ectodermally and endodermally derived epithelia, respectively (Izumi and Furuse, 2014). To date, over 20 *D. melanogaster* pSJ-associated proteins have been identified, and these include transmembrane and cytoplasmic proteins (Izumi and Furuse, 2014; Deligiannaki et al., 2015; Jonusaite et al., 2016a). Loss-of-function mutations in most of these proteins prevent the formation of septa or SJ organization, which in turn disrupts the transepithelial barrier properties of ectodermally derived epithelia (for review, see Izumi and Furuse, 2014; Jonusaite et al., 2016a). In addition, three *D. melanogaster* sSJ-specific membrane proteins, snakeskin (Ssk), mesh and Tsp2A, have recently been discovered (Yanagihashi et al., 2012; Izumi et al., 2012, 2016). All three proteins are localized exclusively in the epithelia of the midgut and Malpighian tubules, where sSJs reside, and are required for the barrier function of the midgut (Izumi et al., 2012, 2016; Yanagihashi et al., 2012).

Gliotactin (Gli) is a single-pass transmembrane protein that belongs to the Neuroligin family of cholinesterase-like adhesion molecules. Gli was the first *D. melanogaster* SJ protein to localize exclusively to occluding regions of the tricellular junction (TCJ), which forms at regions of tricellular contact between three neighboring epithelial cells (Schulte et al., 2003; Gilbert and Auld, 2005). In addition to an extracellular cholinesterase-like domain, Gli contains an intracellular domain with two tyrosine

Department of Biology, York University, Toronto, Ontario, Canada M3J 1P3.

*Author for correspondence (artks@yorku.ca)

S.J., 0000-0002-6514-131X

Received 9 January 2017; Accepted 11 April 2017

Journal of Experimental Biology

Journal of Experimental Biology (2017) 220, 2354-2363 doi:10.1242/jeb.156125

List of abbreviations

BW	brackish water
Dlg	discs large (protein)
EST	expressed sequence tag
FW	freshwater
Gli	gliotactin
pSJ	pleated SJ
SJ	septate junction
sSJ	smooth SJ
Ssk	snakeskin (protein)
TCJ	tricellular junction
TJ	tight junction
VA	V-type H^+-ATPase
βLac	*β-lactamase*

phosphorylation residues and a PDZ binding motif, both conserved in all Gli homologs (Padash-Barmchi et al., 2010). In *D. melanogaster* ectodermal epithelia, Gli is required for the development of both TCJ and SJ (Schulte et al., 2003). Gli-null mutant *D. melanogaster* embryos die because of paralysis resulting from disrupted TCJ and SJ permeability barriers (Schulte et al., 2003). In polarized epithelia, Gli levels and its TCJ localization are tightly regulated via phosphorylation, endocytosis and degradation (Padash-Barmchi et al., 2010). When overexpressed, Gli spreads away from the TCJ into the bicellular SJ domain, where it interacts with the cytoplasmic SJ protein discs large (Dlg) (Schulte et al., 2006; Padash-Barmchi et al., 2010, 2013). Gli interaction with Dlg results in reduced Dlg levels, tissue overgrowth and apoptosis (Schulte et al., 2006; Padash-Barmchi et al., 2010, 2013).

The effect of environmental salinity on the SJ permeability of osmoregulatory epithelia of aquatic insects and, more broadly, invertebrates is not well understood. Salinity-induced changes in the ultrastructure of pSJs have been reported for the gill epithelium of euryhaline crabs (Luquet et al., 1997, 2002). This suggests that alterations in the molecular physiology of aquatic arthropod SJs in osmoregulatory epithelia should be expected in response to changes in the ionic strength of their surroundings, and two recent studies support this hypothesis. The first (Jonusaite et al., 2017) reported that the flux rate of the paracellular permeability marker PEG-400 was greater across the midgut epithelium of BW-reared larval *A. aegypti* when compared with organisms reared in FW, while the Malpighian tubules had reduced PEG-400 permeability in BW versus FW larvae. The changes in PEG-400 flux across the midgut and Malpighian tubules occurred in association with increased transcript abundance of the sSJ proteins Ssk and mesh in these epithelia of BW-reared larvae when compared with FW animals (Jonusaite et al., 2017). In a second study, a salinity-induced increase in the protein abundance of the integral SJ protein kune-kune (Kune) was observed in the posterior midgut as well as anal papillae of *A. aegypti* larva while other SJ proteins were unaltered (Jonusaite et al., 2016b). Taken together, these observations suggest that select SJ proteins contribute to osmoregulatory homeostasis in larval *A. aegypti* (Jonusaite et al., 2016b, 2017).

To the best of our knowledge, an osmoregulatory role for TCJs and the idea that a tricellular SJ protein might contribute to osmoregulatory homeostasis in an aquatic invertebrate have yet to be explored. In aquatic vertebrates such as fishes, the tricellular tight junction (TJ) protein tricellulin has been proposed to play a role in maintaining the barrier properties of osmoregulatory organs such as the gill (Kolosov and Kelly, 2013). Therefore, it seems reasonable to consider that in the functionally analogous occluding junction of an aquatic arthropod facing the same physiological problems as that of an aquatic vertebrate, a tricellular SJ protein may also contribute to salt and water balance. In this regard, it can be hypothesized that in *A. aegypti* larvae, Gli will be salinity responsive in osmoregulatory organs and contribute to changes in the permeability of SJs. To address this further, the objectives of the present study were to examine (1) Gli expression and localization in the osmoregulatory tissues of larval *A. aegypti*, (2) changes in Gli abundance in association with changes in environmental ion levels and (3) whether functional knockdown of *gli* would alter the paracellular permeability of a larval mosquito osmoregulatory epithelium, the midgut.

MATERIALS AND METHODS

Experimental animals and culture conditions

Larvae of *Aedes aegypti* (Linnaeus in Hasselquist 1762) were obtained from a colony maintained in the Department of Biology at York University as previously described (Jonusaite et al., 2016b). Hatched first instar larvae were reared in either FW (approximate composition in μmol l^{-1}: $[Na^+]$ 590; $[Cl^-]$ 920; $[Ca^{2+}]$ 760; $[K^+]$ 43; pH 7.35) or 30% seawater (10.5 g l^{-1} Instant Ocean SeaSalt in FW), which served as the experimental BW treatment. Larvae were fed daily and water of appropriate salinity was changed weekly. Experiments were conducted on fourth instar larvae that had not been fed for 24 h before collection.

Identification of *gli* in *Aedes aegypti* and quantitative real-time PCR (qPCR) analysis

Total RNA was extracted from larval *A. aegypti* tissues (midgut with gastric caecae, Malpighian tubules, hindgut and anal papillae) using TRIzol® reagent (Invitrogen, Burlington, ON, Canada) according to the manufacturer's instructions. Tissues from 50 larvae were pooled per one biological sample. All RNA samples were treated with the TURBO DNA-*free*™ kit (Ambion, Life Technologies, Burlington, ON, Canada) and template cDNA was synthesized using the iScript™ cDNA synthesis kit as per the manufacturer's instructions (Bio-Rad, Mississauga, ON, Canada). Expressed sequence tags (ESTs) from *A. aegypti* genome that were similar to *D. melanogaster gli* (GenBank accession number AAC41579) were sought using the National Center for Biotechnology Information (NCBI) database BLAST search engine. Newly identified ESTs were confirmed to be protein encoding using a reverse xBLAST. A reading frame was established using BLASTn alignment and ORF Finder (http://www.ncbi.nlm.nih.gov/gorf/). A primer set for *gli* was designed based on EST sequences using Primer3 software (v. 0.4.0): forward 5′-TCGGCATAGACAACA-ACGTC-3′, reverse 5′-CGTAGCGAGCTTTGACTTCC-3′; amplicon size 1182 bp; annealing temperature 59°C. Expression of mRNA encoding *gli* in the whole body and osmoregulatory tissues of *A. aegypti* larvae was examined by routine reverse transcriptase PCR (RT-PCR). *18S rRNA* mRNA abundance was used as a loading control and was amplified using primers previously described (Jonusaite et al., 2016b). Resulting RT-PCR amplicons were resolved by agarose gel electrophoresis and sequence identities were confirmed after sequencing at the York University Core Molecular Facility (Department of Biology, York University, ON, Canada). The amplified *A. aegypti gli* sequence was confirmed using a BLAST search and submitted to GenBank (accession number KX823345). ClustalW software was used to align the amino acid sequence of *A. aegypti* Gli with that of *D. melanogaster*. *In silico* analysis of the *A. aegypti* Gli amino acid sequence was performed using EXPASY PROSITE (posttranslational modifications and protein domains), ProtParam

Journal of Experimental Biology (2017) 220, 2354-2363 doi:10.1242/jeb.156125

(protein weight and stability parameters such as predicted half-life), and ProtScale and TMHMM (hydrophobicity scale and transmembrane domains). Final *A. aegypti* Gli topography was visualized using TOPO2 software.

Transcript abundance of *gli* in the midgut, Malpighian tubules, hindgut and anal papillae of *A. aegypti* larvae was examined by qPCR analysis. Reactions were carried out using the primers listed above and SYBR Green I Supermix (Bio-Rad Laboratories, Mississauga, ON, Canada) with a Chromo4™ Detection System (CFB-3240, Bio-Rad Laboratories Canada) under the following conditions: one cycle of denaturation (95°C, 4 min) followed by 40 cycles of denaturation (95°C, 30 s), annealing (59°C, 30 s) and extension (72°C, 30 s). For qPCR analyses, *gli* mRNA abundance was normalized to either *18S rRNA* or *rp49* transcript abundance. *Aedes aegypti 18S rRNA* and *rp49* mRNA were amplified using primers previously described (Jonusaite et al., 2016b).

Western blot analysis and immunohistochemistry

Western blotting for Gli in the tissues of interest (gastric caecae, anterior midgut, posterior midgut, Malpighian tubules, hindgut and anal papillae) was performed as previously detailed (Jonusaite et al., 2016b). A custom-made polyclonal antibody that was produced in rabbit against a custom-made synthetic peptide (GASRAGYDRSNNAS) corresponding to a 14-amino acid region of the C-terminal cytoplasmic tail of *A. aegypti* Gli (GenScript USA, Piscataway, NJ, USA) was used at 1:500 dilution. To confirm the specificity of the custom-made *A. aegypti* Gli antibody, a comparison blot was also run with the Gli antibody pre-absorbed with 10× molar excess of the immunogenic peptide for 1 h at room temperature prior to application to blots. After examination of Gli expression, blots were stripped and re-probed with a 1:200 dilution of mouse monoclonal anti-JLA20 antibody (J. J.-C. Lin, Developmental Studies Hybridoma Bank, Iowa City, IA, USA) for actin. Densitometric analysis of Gli and actin was conducted using ImageJ 1.47 software (National Institutes of Health, Bethesda, MD, USA). Gli abundance was expressed as a normalized value relative to the abundance of the loading control.

Immunohistochemical localization of Gli in whole-mount guts and paraffin sections of anal papillae was conducted according to previously described protocols (see Jonusaite et al., 2013, 2016b) using a 1:50 dilution of the custom-made anti-Gli antibody described above. Whole-mount guts and paraffin sections of anal papillae were also treated with a 1:1000 dilution of a rabbit polyclonal anti-*Ae*AE antibody for the SLC4-like anion exchanger (a kind gift from Dr P. M. Piermarini, Department of Entomology, The Ohio State University, Wooster, OH, USA) and a 1:100 dilution of a mouse polyclonal anti-ATP6V0A1 antibody for V-type H^+-ATPase (VA; Abnova, Taipei, Taiwan), respectively. A goat anti-rabbit antibody conjugated to Alexa Fluor 594 (Jackson Immunoresearch) was used at 1:400 to visualize Gli and *Ae*AE, and a sheep anti-mouse antibody conjugated to Cy-2 (Jackson Immunoresearch) was applied at 1:400 to visualize VA. Negative control slides were also processed as described above with either primary antibodies omitted or the Gli antibody pre-absorbed with 10× molar excess of the immunogenic peptide for 1 h at room temperature prior to application to tissues. Images of sections of anal papillae were captured using an Olympus IX71 inverted microscope (Olympus Canada, Richmond Hill, ON, Canada) equipped with an X-CITE 120XL fluorescent Illuminator (X-CITE, Mississauga, ON, Canada). Whole-mounts were examined using an Olympus BX-51 laser-scanning confocal microscope. Images were assembled using Adobe Photoshop CS2 software (Adobe Systems Canada, Toronto, ON, Canada).

dsRNA preparation and delivery

Total RNA was extracted from the midguts of fourth instar *A. aegypti* larvae and cDNA was generated as described above. Using this cDNA template, a fragment of the *gli* gene (976 bp) was amplified by RT-PCR using primers (forward 5′-TGCTCAATC-GAAACTTCGTG-3′; reverse 5′-GTTCCCACCAGAACTCCGT-A-3′) designed based on the *gli* sequence submitted to GenBank. A BLAST search analysis was used to confirm the absence of sequence identity between the 976 bp *gli* gene fragment and other genes found in *A. aegypti*. A fragment of *β-lactamase* (*βLac*; 799 bp) was also amplified by RT-PCR from a pGEM-T-Easy vector (kind gift from J. P. Paluzzi, York University) using the following primers: forward 5′-ATTTCCGTGTCGCCCTTATTC-3′; reverse 5′-CGTTCATCCATAGTTGCCTGAC-3′. PCR products were concentrated and purified using a QIAquick PCR Purification kit (Qiagen, Toronto, ON, Canada) and used to generate double-stranded (ds) RNAs by *in vitro* transcription using the Promega T7 RiboMAX Express RNAi Kit (Promega, Madison, WI, USA). dsRNA was delivered to larvae as previously described (Chasiotis et al., 2016) with slight modification. Briefly, groups of 25 4th instar larvae were incubated for 4 h in 500–600 µl PCR-grade water containing 0.5 µg $µl^{-1}$ dsRNA and then transferred into 20 ml distilled water. To confirm reduction in *gli* transcript as a result of dsRNA treatment, total RNA was extracted and cDNA generated from larval whole body and midgut at day 1 post-dsRNA treatment. The latter cDNA templates were used in RT-PCR with the above primers. Reduction in Gli in larval midgut as a result of dsRNA treatment was examined by western blotting at days 1 and 2 post-dsRNA treatment.

Transepithelial PEG-400 flux across the midgut of *A. aegypti*

Flux of the paracellular permeability marker [^{3}H]polyethylene glycol (molecular mass 400 Da; ‘PEG-400’; American Radiolabeled Chemicals, St Louis, MO, USA) across the midgut epithelium of larval *A. aegypti* was determined as previously described (Jonusaite et al., 2017). [^{3}H] PEG-400 flux rates were determined from larvae treated with *gli* or *βLac* dsRNA.

Statistics

Data are expressed as means±s.e.m. (n). Comparisons between tissues were assessed with a one-way ANOVA followed by a Tukey’s comparison test. A Student’s t-test was used to examine for significant differences between control and experimental groups. Statistical significance was allotted to differences with $P<0.05$. All statistical analyses were conducted using SigmaStat 3.5 software (Systat Software, San Jose, USA).

RESULTS

Gli identification and expression in larval *A. aegypti*

Using the NCBI EST database, a full coding sequence of the *A. aegypti* SJ gene *gli* was obtained and primers were designed to amplify regions within and across ESTs using larval cDNA. Assembled sequence identity was confirmed by performing a BLAST search using the amplified coding sequence of *gli*. *Aedes aegypti* Gli encodes a 993 amino acid protein with a predicted molecular weight of 113 kDa that shares 68% amino acid identity with *D. melanogaster* Gli (Fig. 1A). The primary structure of *A. aegypti* Gli is similar to that of *D. melanogaster* Gli (Padash-Barmchi et al., 2010) and contains a single-pass transmembrane

Journal of Experimental Biology (2017) 220, 2354-2363 doi:10.1242/jeb.156125

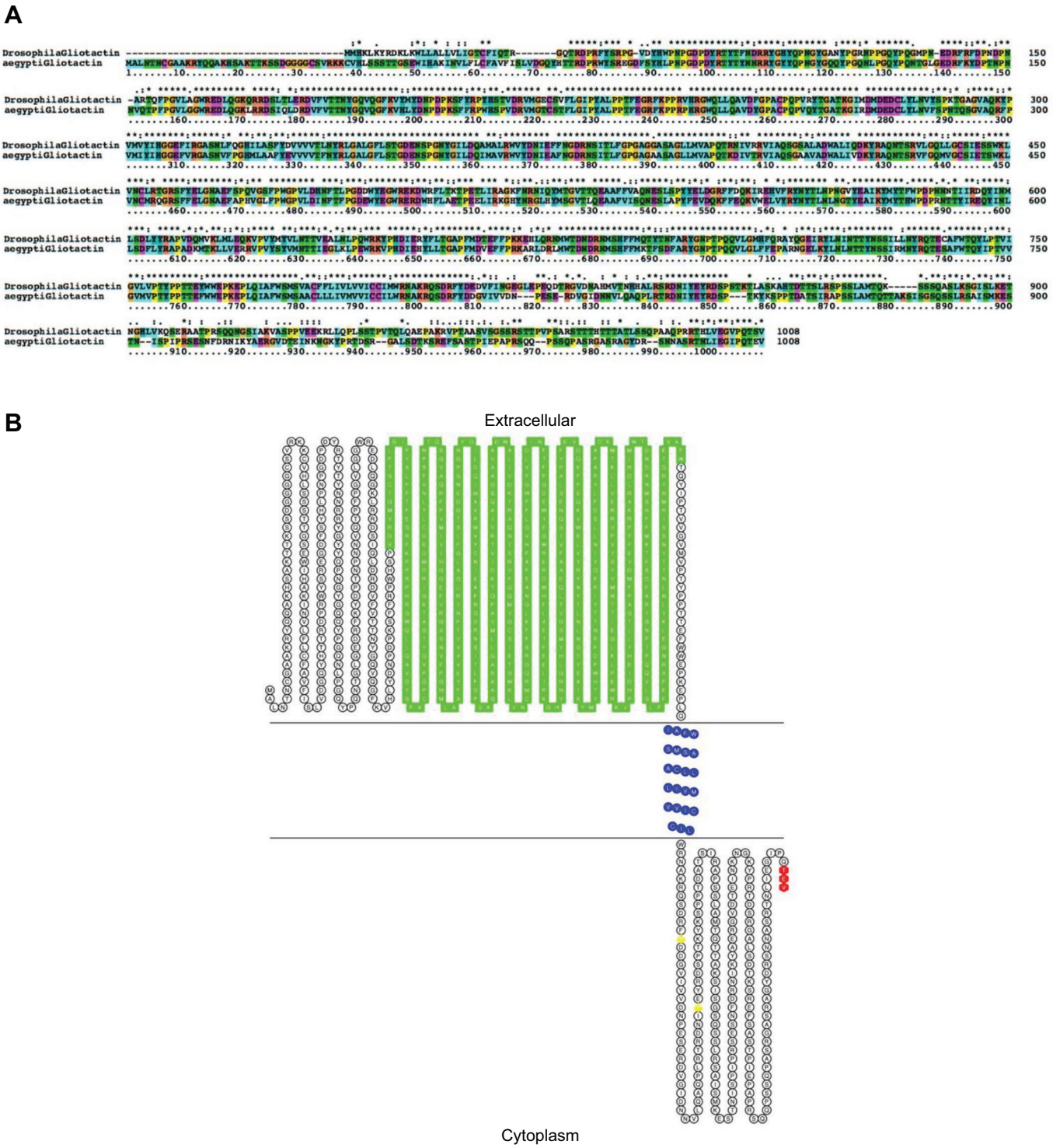

Fig. 1. Annoted amino acid sequence of *Aedes aegypti* gliotactin (Gli). (A) The amino acids of *A. aegypti* Gli were aligned with those of *Drosophila melanogaster* (accession no. AAC41579) using the ClustalW algorithm. Asterisk (*) represents identical amino acid residues shared between *A. aegypti* Gli and *D. melanogaster* Gli, colon (:) indicates conservation between two amino acid residues of strongly similar properties and period (.) indicates conservation between two amino acid residues of weakly similar properties. (B) *Aedes aegypti* Gli has a single-pass transmembrane domain (blue), an extracellular region containing a carboxylesterases type-B domain (green), and an intracellular domain with two highly conserved tyrosine phosphorylation residues (yellow) and a PDZ binding motif (red).

domain, a large extracellular region containing a carboxylesterase type-B domain, and an intracellular domain with two tyrosine phosphorylation residues and a PDZ binding motif (Fig. 1B).

Quantitative analysis of *gli* mRNA in the osmoregulatory organs of *A. aegypti* larvae revealed the presence of *gli* transcript in all tissues examined, i.e. the midgut, Malpighian tubules, hindgut and anal papillae, but transcript abundance was highest in the midgut (Fig. 2A). Western blot analysis of Gli in larval osmoregulatory tissues showed that anti-Gli antibody detected three tissue-specific bands with molecular weights of ~115, ~150

Journal of Experimental Biology

Journal of Experimental Biology (2017) 220, 2354-2363 doi:10.1242/jeb.156125

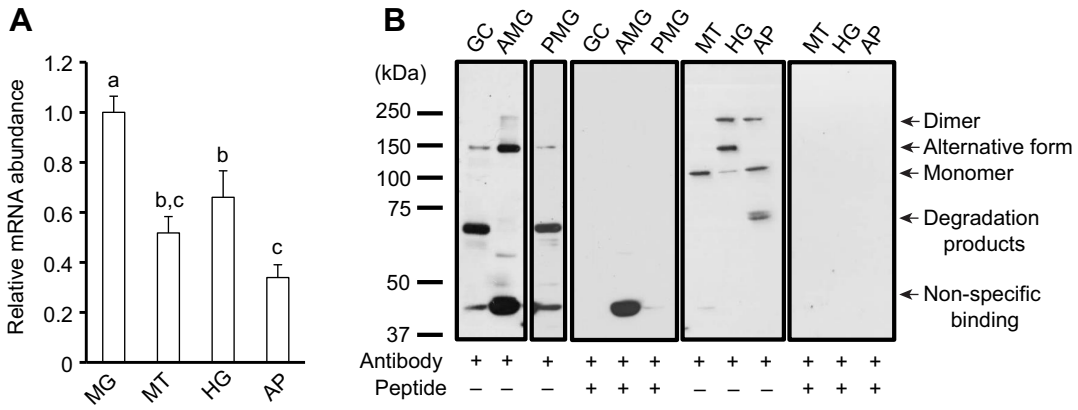

Fig. 2. Gli transcript and protein expression profile in the osmoregulatory tissues of *Aedes aegypti* larvae as determined by qPCR and western blot analysis, respectively. (A) Each gene was normalized to *18S* and was expressed relative to its levels in the midgut (assigned a value of 1). Data are expressed as means±s.e.m. (n=6). Different letters denote statistically significant differences between tissues (one-way ANOVA, Tukey's multiple comparison, P<0.05). (B) Representative western blot of Gli in the osmoregulatory organs of larval *A. aegypti* reveals the presence of Gli monomer at ∼115 kDa, potential dimer at ∼245 kDa, an additional Gli form of ∼150 kDa and some degradation products. In GC, AMG and PMG, an additional band of low molecular weight was detected which was not blocked by antibody pre-absorption with the immunizing peptide. MG, midgut; MT, Malpighian tubules; HG, hindgut; AP, anal papillae; GC, gastric caecae; AMG, anterior midgut; PMG, posterior midgut.

and ∼245 kDa (Fig. 2B). A single ∼115 kDa band, which corresponds to the predicted Gli protein size, resolved in the Malpighian tubules. The protein of ∼115 kDa was also detected in the anal papillae, where an additional putative Gli dimer of ∼245 kDa and a lower molecular mass band (<75 kDa), which most likely represents a degradation product, were seen. Antibody pre-absorption with the immunogenic peptide produced no staining of Gli in the anal papillae (Fig. 2B, right lane). In the hindgut, three Gli products were immunodetected, corresponding to the monomer, dimer and an additional Gli form of ∼150 kDa, which were all blocked by antibody pre-absorption with the immunogenic peptide (Fig. 2B). In the gastric caecae and posterior midgut, Gli was detected as a ∼150 kDa protein and a degradation product, whereas anterior midgut samples revealed the presence of a faint Gli dimer and a predominant ∼150 kDa form (Fig. 2B). A non-specific low molecular weight band (<50 kDa), which was not blocked by the immunogenic peptide, was seen in the samples from different regions of the midgut (Fig. 2B).

Immunostaining of Gli revealed its localization to the entire SJ domain between the epithelial cells of the gastric caecae, and anterior and posterior midgut (Fig. 3A–D). In the Malpighian tubules, Gli immunolocalization appeared to be restricted to the cell–cell contact regions between the stellate and principal cells in the distal two-thirds of the tubule (Fig. 3E–H). Little to no immunoreactivity of Gli was seen in the proximal third of the tubule (Fig. 3H), which appears to lack stellate cells (Patrick et al., 2006; Linser et al., 2012). In addition, Gli immunostaining in the Malpighian tubules was similar to that of an established stellate cell marker *Ae*AE (Fig. 3I-K; Piermarini et al., 2010; Linser et al., 2012). Because both Gli and *Ae*AE antibodies were produced in rabbits, double labeling could not be performed. In the whole-mount rectum and sections of anal papillae, Gli showed some punctuate staining along the plasma membranes of the rectal epithelial cells (Fig. 3M) and papilla epithelium (Fig. 3N). Within the epithelium of anal papillae, there was some overlap in immunoreactivity between Gli and apical membrane marker VA (Fig. 3O). Gli staining was absent in control whole mounts or sections which were probed with secondary antibodies only or with Gli antibody that was pre-absorbed with the immunogenic peptide (Fig. 3P; only sections of anal papillae are shown). Gli was not observed to immunolocalize in non-epithelial tissue where SJs have not been described, such as the musculature of the gut (Fig. 3B,C).

Effects of rearing salinity on *gli* transcript and Gli protein abundance

Rearing the larvae of *A. aegypti* in BW resulted in a significant increase in *gli* mRNA abundance as well as Gli protein abundance in the midgut and Malpighian tubules (Fig. 4). Because of the lack of consistent immunodetection of Gli in the posterior midgut, Gli protein abundance was examined only in the anterior midgut of FW- and BW-reared animals. Elevated Gli protein abundance was also observed in the hindgut of BW-reared larvae, with no change in *gli* transcript abundance in this tissue compared with FW-reared animals (Fig. 4). While the ∼150 kDa Gli form was always detected in the samples of anterior midgut and hindgut from FW- and BW-reared animals, the potential dimer form was not consistently detected in these tissues. As a result, only the ∼150 kDa Gli form was quantified in these tissues of FW- and BW-reared larvae.

Lastly, there was no change in *gli* transcript and Gli protein monomer and putative dimer abundance in the anal papillae when larvae were reared in BW (Fig. 4).

Effect of Gli dsRNA knockdown on midgut permeability

To characterize Gli function in the osmoregulatory epithelia of larval *A. aegypti*, *gli* expression was knocked down using *gli*-targeting dsRNA. Following this, Gli protein abundance was examined as well as paracellular permeability in the midgut using the midgut permeability assay (see Jonusaite et al., 2017). Larvae treated with *gli* dsRNA showed a significant reduction in ∼150 kDa Gli protein abundance in the anterior midgut at day 2 post-*gli* dsRNA treatment compared with the group treated with *βLac* dsRNA (Fig. 5A,B). As such, day 2 post-*gli* dsRNA treated larvae were subjected to the midgut permeability assay. These larvae

Journal of Experimental Biology (2017) 220, 2354-2363 doi:10.1242/jeb.156125

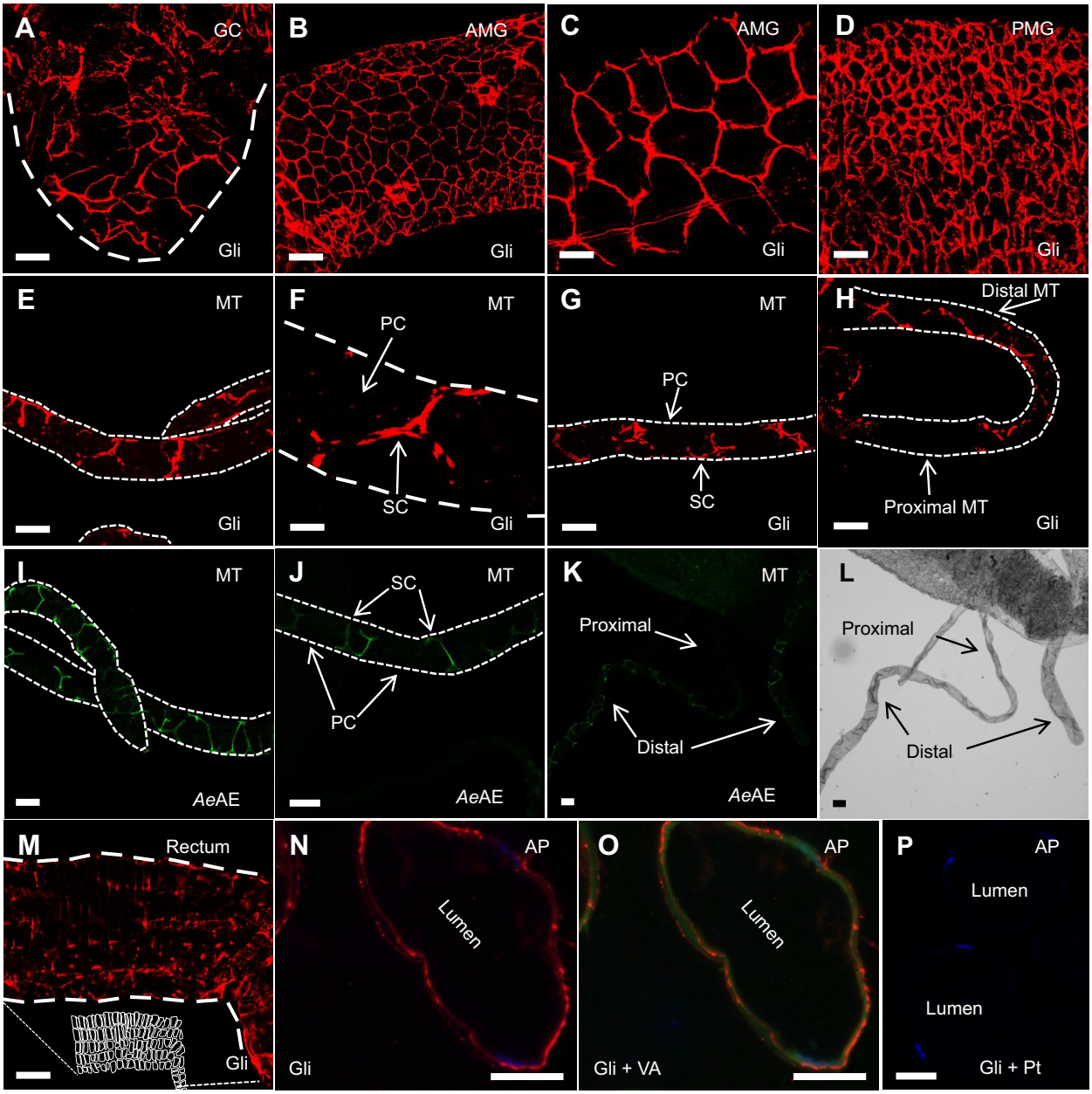

Fig. 3. Immunofluorescence staining of Gli in the osmoregulatory tissues of *Aedes aegypti* larva. Gli was localized to regions of cell–cell contact between the epithelial cells of the gastric caecae (A), and anterior and posterior midgut (B–D). In the Malpighian tubules, Gli immunostaining appears to be confined to the contact regions between the stellate and principal cells (SC and PC, respectively; arrows in F and G) in the distal two-thirds of the tubule (E–H) as compared with the expression of the stellate cell marker *Ae*AE (I–K, green). (L) Brightfield image of K. Gli also shows some discontinuous immunostaining along the plasma membranes of the epithelial cells in the rectum (M; shown also are outlined rectal cell boarders) and anal papillae epithelium (N), where it exhibits some co-immunoreactivity with apical V-type H^+-ATPase (VA; O, green). Nuclei of anal papilla epithelium are stained with DAPI (blue) in N. (P) Control sections of anal papillae treated with anti-Gli antibody in the presence of immunizing peptide (Pt) and only DAPI (blue) staining is observed. Scale bars: (A,C,D,F) 20 µm, (B,E,G–K,L,M–P) 50 µm. GC, gastric caecae; AMG, anterior midgut; PMG, posterior midgut; MT, Malpighian tubules; AP, anal papillae.

exhibited decreased PEG-400 flux (efflux, basolateral to apical) across the midgut compared with values from midguts of animals treated with *βLac* dsRNA (Fig. 5C).

DISCUSSION

Overview

In this study, we identified the *A. aegypti* homolog of the transmembrane SJ protein Gli. We hypothesized that Gli would localize to the TCJ complex in the epithelia of larval mosquito, as has previously been reported in *D. melanogaster* (see Schulte et al., 2003, 2006); however, this was not the case as in most tissues examined, Gli localized at bicellular SJs. In contrast, the hypothesis that Gli expression would respond to alterations in salinity can be accepted as Gli levels were found to exhibit an organ-specific increase in animals reared in BW. Furthermore, the hypothesis that Gli would contribute to changes in the permeability of SJs in association with salinity change is supported by changes in paracellular permeability of the midgut epithelium (as measured by PEG-400 flux), which decreased following a dsRNA targeted reduction in Gli abundance. These observations suggest that Gli

Journal of Experimental Biology (2017) 220, 2354-2363 doi:10.1242/jeb.156125

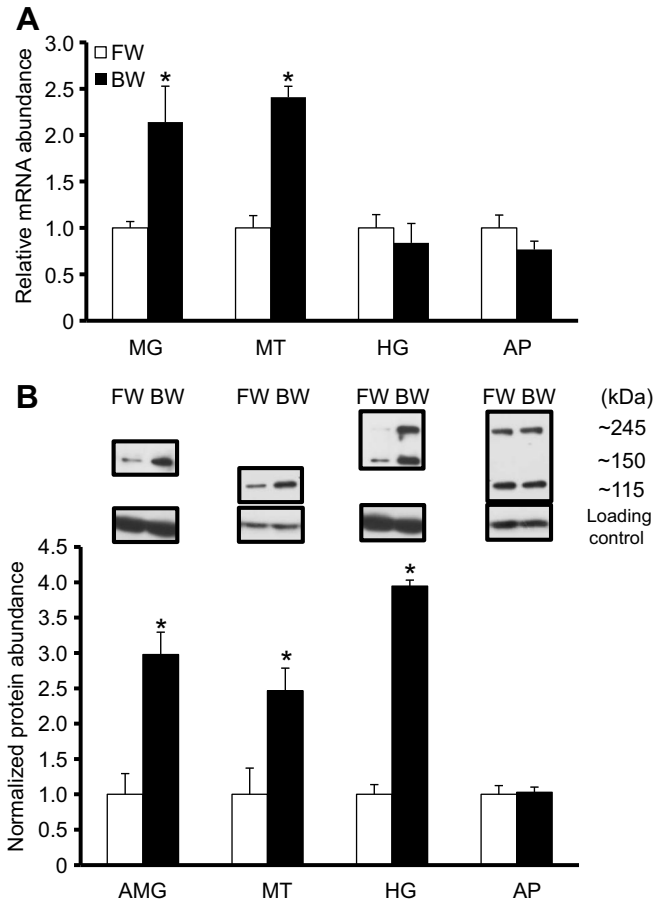

Fig. 4. The effect of rearing salinity on Gli transcript and normalized protein abundance in the osmoregulatory tissues of *Aedes aegypti* larvae as examined by qRT-PCR and western blot analysis, respectively. (A) Gli transcript abundance. Each gene was normalized to *rp49* and expressed relative to its freshwater (FW) value (assigned value of 1). (B) Normalized protein abundance. Representative western blots of Gli are ~115, 150 and ~245 kDa bands, loading control is actin. Data are expressed as means±s.e.m. (n=3–6). Asterisks denote a significant difference from FW (Student's t-test, *P<0.05). MG, midgut; MT, Malpighian tubules; HG, hindgut; AP, anal papillae; BW, brackish water; AMG, anterior midgut.

participates in the maintenance of salt and water balance and contributes to the regulation of paracellular permeability of osmoregulatory epithelia in the aquatic *A. aegypti* larvae. In addition, this study makes important observations that set the stage for consideration of, in further detail, what functional similarities and/or differences exist between Gli homologs within the SJ complex in the osmoregulatory epithelia of aquatic and non-aquatic insects.

Gli expression and localization in the osmoregulatory organs of larval mosquitoes

An expression profile of mRNA encoding Gli revealed its presence in all larval *A. aegypti* organs examined in this study, i.e. the midgut, Malpighian tubules, hindgut and anal papillae. However, the midgut showed significantly elevated levels of Gli transcript (Fig. 2A). The expression of Gli in a wide range of epithelial tissues, including the midgut and hindgut, has been shown in larval *D. melanogaster* (Schulte et al., 2003, 2006; Byri et al., 2015). In contrast, Gli is not expressed in the *D. melanogaster* Malpighian tubules (Schulte et al., 2006). As such, our observation of Gli transcript in the tubules of *A. aegypti* larvae (see Fig. 2A) suggests organ-specific differences in the molecular composition of SJs between the two dipteran species. Support for this idea comes from our recent study reporting the expression of the SJ protein Kune in the posterior midgut of larval *A. aegypti* (Jonusaite et al., 2016b). In *D. melanogaster*, Kune is found in pSJ-bearing ectodermal epithelia such as the foregut and hindgut, but not in the sSJ-bearing endodermal midgut epithelium (Nelson et al., 2010).

Consistent with *gli* transcript expression, Gli protein was detected in all osmoregulatory organs of *A. aegypti* larvae by western blotting. In addition, tissue-specific forms of Gli were revealed. A single Gli immunoreactive band of ~115 kDa, consistent with an expected molecular mass of ~113 kDa, resolved in the Malpighian tubules (Fig. 2B). A Gli monomer was also found in anal papillae, where an additional higher molecular mass band of ~245 kDa, which is approximately twice the weight of a Gli monomer, was observed, and we interpret this to be a Gli dimer. The vertebrate homologs of Gli, neuroligins, have been shown to dimerize or oligomerize via their extracellular serine esterase-like domain (Ichtchenko et al., 1995, 1996), and Gli dimerization has also been suggested for *D. melanogaster* (Venema et al., 2004; Padash-Barmchi et al., 2013). In contrast, we can not rule out the possibility that the observed ~245 kDa Gli band may be a product of a Gli heterodimer complex with another SJ protein such as Dlg, which has been shown to occur in adult *D. melanogaster* (Schulte et al., 2006).

In the present study, bands corresponding to Gli monomer, putative dimer and an additional form at ~150 kDa were detected in the hindgut of *A. aegypti* larvae (Fig. 2B). One explanation for the presence of the Gli immunoreactive band at ~150 kDa, which is ~35 kDa greater than the monomer, is that it may represent a post-translationally modified Gli form. The cytoplasmic domain of all Gli homologs, including that of *A. aegypti*, has two strongly conserved tyrosine phosphorylation sites (Fig. 1) (Padash-Barmchi et al., 2010) and in *D. melanogaster*, the expression level of Gli and unique localization to the TCJ are regulated through phosphorylation and subsequent endocytosis (Padash-Barmchi

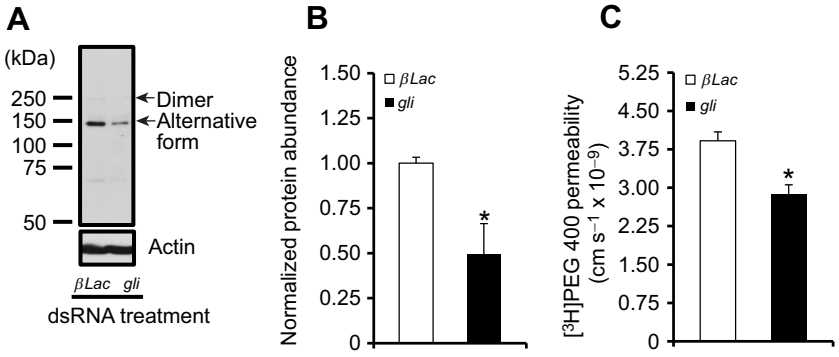

Fig. 5. The effects of *gli* dsRNA treatment on Gli abundance and [^{3}H]PEG-400 movement across the midgut of *Aedes aegypti* larvae. (A) Representative western blot and (B) densitometric analysis of ~150 kDa Gli form in larval anterior midgut (n=3), and (C) measurements of PEG-400 flux across the entire larval midgut (n=13 for *βLac* and n=17 for *gli*) on day 2 following control *β-lactamase* (*βLac*) or *gli*-targeting dsRNA treatment. Gli abundance was normalized to actin and expressed relative to the *βLac* group. Data are expressed as means±s.e.m. Asterisks indicate a significant difference from the *βLac* group (Student's t-test, *P<0.05).

Journal of Experimental Biology (2017) 220, 2354-2363 doi:10.1242/jeb.156125

et al., 2010, 2013). Tight control of Gli is necessary, as its displacement away from the TCJ throughout the SJ domain leads to delamination, migration and apoptosis of columnar epithelial cells in imaginal discs (Padash-Barmchi et al., 2010, 2013). As shown in the present study, the predominant ∼150 kDa Gli band was also detected throughout the midgut of larval *A. aegypti*, i.e. the gastric caecae, anterior and posterior midgut (Fig. 2B). If ∼150 kDa band is a product of post-translationally modified Gli, it is reasonable to suggest that *A. aegypti* Gli is phosphorylated, as it is the case for *D. melanogaster* Gli (Padash-Barmchi et al., 2010, 2013). However, phosphorylation alone is unlikely to cause an increase in Gli protein by ∼35 kDa, suggesting that other biochemical processes also play a role. Interestingly, using an *in silico* NetNGlyc analysis (Gupta et al., 2004), four putative sites of *N*-glycosylation of *A. aegypti* Gli protein were identified (data not shown). A ∼30 kDa shift in the molecular mass has been shown to result from the *N*-glycosylation of *A. aegypti* transporter protein *Ae*AE when expressed heterologously in *Xenopus* oocytes (Piermarini et al., 2010). Our bioinformatics analysis of *A. aegypti* Gli did not suggest the presence of Gli splice variants, and the nature of the ∼150 kDa Gli form in larval *A. aegypti* remains to be determined in future biochemical studies.

Localization of Gli revealed its presence at the cell–cell contact regions between the epithelial cells of gastric caecae, anterior and posterior midgut (Fig. 3A–D), suggesting that Gli is a component of bicellular SJs in these epithelia of larval *A. aegypti*. This observation is inconsistent with *D. melanogaster* Gli, which is reported to be concentrated at the TCJs in the midgut epithelium (Byri et al., 2015). However, in the epithelia of epidermis and wing imaginal discs, *D. melanogaster* Gli spreads throughout the entire SJ domain and interacts with other bicellular SJ components when overexpressed (Schulte et al., 2006). As mentioned above, the presence of Gli at the bicellular SJs in *D. melanogaster* epithelia results in tissue overgrowth and apoptosis (Padash-Barmchi et al., 2010, 2013). Hence, it is interesting to consider our observations, made in this study, of Gli localization to the bicellular SJs throughout the midgut of larval *A. aegypti* (see Figs 2B and 3A–D). It appears that differences in junctional localization of Gli exist between the two species. This idea is further supported by the finding of Gli in the Malpighian tubules of *A. aegypti* larvae (present study) and its absence from *D. melanogaster* tubules (Schulte et al., 2003, 2006). We found that Gli immunostaining appeared to be concentrated at the cell–cell contact regions between the principal and stellate cells of larval *A. aegypti* tubules, in particular when Gli staining is compared with the staining for the stellate cell marker *Ae*AE (Fig. 3E–K). The sSJ-specific proteins Ssk and mesh have recently been found in the Malpighian tubules of *A. aegypti* larvae, where they localize to SJs between all cells (see Jonusaite et al., 2017). Taken together, it is reasonable to suggest that there is a difference in the molecular architecture of SJs between the stellate-principal cells and principal-principal cells in the Malpighian tubules of larval *A. aegypti*. The presence of cell-type-specific SJ proteins in larval mosquito tubules could be expected given that in dipterans, the principal and stellate cells are derived from the two different embryonic layers, the ectoderm and the mesoderm, respectively (Beyenbach et al., 2010; Clements, 1992).

Lastly, our immunohistochemical analysis of Gli in the hindgut and anal papillae of *A. aegypti* larvae revealed its discontinuous immunostaining along the plasma membranes of rectal epithelial cells (Fig. 3M) and the syncytial papilla epithelium, where Gli showed some co-localization with the apically expressed VA (Fig. 3N,O). In the embryonic hindgut of *D. melanogaster*, Gli is restricted to the TCJ domain between the epithelial cells (Schulte et al., 2003). However, patchy Gli staining in the epithelial cells of the dorsal epidermis has been reported for *D. melanogaster* embryos (Schulte et al., 2003). The finding of Gli in the anal papilla epithelium of larval *A. aegypti* (present study), which lacks SJs (Sohal and Copeland, 1966; Edwards and Harrison, 1983), suggest a non-junctional role for Gli in this tissue, as has been suggested for Kune (Jonusaite et al., 2016b). In *D. melanogaster*, Gli is also required for parallel alignment of wing hairs in the adult wing epithelium, and this Gli function is dependent on its localization to the apical cell membranes (Venema et al., 2004). Evidence for a non-junctional role for SJ proteins also comes from a finding that a cell adhesion molecule Fasciclin 2 (Fas2), which is known to localize to SJs in the Malpighian tubules of late-stage *D. melanogaster* embryos, switches its localization to the apical membrane of the principal cells in larval and adult flies where it elicits effects on microvillus length and organization as well as tubule transport capacity (Halberg et al., 2016).

The response of Gli to BW rearing

In the present study, we report that an increase in external salt content triggered organ-specific changes in Gli transcript and protein abundance in *A. aegypti* larvae. Rearing larvae in BW resulted in an increase in Gli protein abundance in the anterior midgut and Malpighian tubules, which was consistent with increased Gli transcript levels in these organs (Fig. 4A,B). In addition, there was significantly higher Gli protein abundance in the hindgut of BW-reared larvae compared with FW animals, albeit with no change in transcript abundance (Fig. 4A,B). Lack of correlation between mRNA transcript and protein abundance has been recently reported for *A. aegypti* Kune (Jonusaite et al., 2016b), and such a phenomenon may occur as a result of mRNA-regulatory mechanisms or differences in protein degradation rate (Fournier et al., 2010). Indeed, in addition to tight control of *D. melanogaster* Gli protein levels by tyrosine phosphorylation and endocytosis (Padash-Barmchi et al., 2010, 2013), Gli levels are also regulated at the mRNA level by microRNA-mediated degradation (Sharifkhodaei et al., 2016). Our observation of increased Gli abundance in *A. aegypti* larval anterior midgut and Malpighian tubules in response to salinity (see Fig. 4B) coincides with greater transcript abundance of Ssk and mesh in the midgut and Malpighian tubules and Kune protein abundance in the posterior midgut of BW-reared larvae when compared with FW-reared animals (Jonusaite et al., 2016b, 2017). If Gli is required for the formation of the paracellular barrier in the midgut, Malpighian tubules and hindgut of larval *A. aegypti*, as it is in *D. melanogaster* salivary gland epithelium (Schulte et al., 2003), it could be suggested that increased Gli protein abundance observed in BW-reared larvae will lead to decreased paracellular permeability of these epithelia under saline conditions. Indeed, the Malpighian tubules of BW-reared larvae exhibit a lower flux rate of the paracellular permeability marker PEG-400 (Jonusaite et al., 2017). However, this does not appear to be the case in the midgut, which becomes more permeable to PEG-400 when *A. aegypti* larvae are reared in BW (Jonusaite et al., 2017). Together, these observations suggest that Gli may have organ-specific functions, and in addition to playing a role in the barrier function of SJs, Gli may contribute to a paracellular channel function, i.e. the ability of SJs to selectively allow paracellular transport of molecules of a certain size or charge or both. Nevertheless, and in contrast to the response of Gli in the epithelia of the gut to BW

Journal of Experimental Biology (2017) 220, 2354-2363 doi:10.1242/jeb.156125

conditions, there was no change in Gli transcript and protein abundance in the anal papillae of BW-reared *A. aegypti* larvae compared with FW animals (Fig. 4A,B). The role of Gli in the papillae epithelium is unclear at this stage, but its lack of response to salinity is in contrast to Kune, which was previously shown to be significantly elevated in this tissue upon BW rearing (Jonusaite et al., 2016b).

Gli dsRNA knockdown and midgut epithelium permeability

To further explore the idea that an increase in Gli abundance may contribute to an increase in SJ permeability in the midgut, a loss of function approach was taken by targeting *gli* for knockdown using dsRNA. Knockdown of *gli* resulted in a reduction in anterior midgut Gli protein abundance as well as a corresponding, and significant, decrease in PEG-400 flux across the midgut (Fig. 5). From a functional standpoint, these observations are consistent with the aforementioned increase in paracellular permeability that occurs when Gli abundance is increased in BW-reared larvae, suggesting that Gli is required for enhanced paracellular permeability or channel function of midgut SJs. In the TJ complex of vertebrate epithelia, the importance of select TJ proteins imparting channel or pore function is well documented (for review, see Günzel and Yu, 2013). More specifically, a key role in determining the permeability properties of vertebrate epithelial cells is played by the transmembrane TJ proteins claudins, which can either contribute to or dictate the barrier or channel/pore properties of an epithelium. In the case of the latter, select claudins are able to contribute to an increase in the permeability of certain ion species or molecules of a certain size (Günzel and Yu, 2013). In invertebrates, it has been demonstrated that the sSJs in the midgut epithelium of lepidopteran *Bombyx mori* larvae display a high selectivity with respect to the size and the charge of permeating ions (Fiandra et al., 2006). But to our knowledge, no study has linked specific elements of the SJ complex with this kind of physiological process in invertebrate epithelia. The questions of how Gli contributes to increased junctional permeability in the midgut of larval *A. aegypti*, as reported in this study, and what these junctions are more permeable to when larvae are in BW remain to be answered. But it could be speculated that Gli might contribute to water transport across the midgut of *A. aegypti* larvae. For example, *A. aegypti* larvae have been shown to greatly increase drinking rates under BW conditions (Edwards, 1982; Clements, 1992). Increased selective paracellular midgut permeability to water movement from the midgut lumen into the hemolymph would help maintain body volume while simultaneously limiting salt loading from ingested saline medium. The participation of claudin TJ proteins in water-selective movement across vertebrate epithelia has been described in the vertebrate kidney proximal tubule (Rosenthal et al., 2010). Alternatively, Gli might play a role in the formation of ion-selective SJs in larval *A. aegypti*, as has been recently suggested for Ssk and mesh (Jonusaite et al., 2017). More specifically, it has been proposed that Ssk and mesh might facilitate paracellular Cl^- movement in the midgut and Malpighian tubules in response to salinity (Jonusaite et al., 2017). Given that *A. aegypti* larvae reared in BW show elevated Gli protein levels together with increased Ssk and mesh transcript abundance in the midgut and Malpighian tubules (see Fig. 4B and Jonusaite et al., 2017), it seems reasonable to suggest that all three SJ proteins are functionally involved in the maintenance of salt and water balance in BW-reared *A. aegypti* larvae, but whether they share a similar role in the SJ function, such as modulating Cl^- conductance, remains to be investigated. Regardless of the mechanism, the results are in agreement with our hypothesis that Gli plays a role in the regulation of the permeability properties of the osmoregulatory epithelia in larval *A. aegypti*.

Perspectives and significance

Studies performed in *D. melanogaster* have greatly expanded our knowledge of the molecular components of insect SJs. Yet, we are still far from understanding the molecular physiology of SJs in other invertebrate species and in particular, how SJ barrier properties either impede solute movement or act as a selectively permeable secretory pathway. In addition, how the SJ integrates and modulates its properties in different epithelia and under different physiological, as well as environmental, conditions remains poorly understood. Recent studies on larval mosquitoes (Jonusaite et al., 2016b, 2017) have pointed toward a dynamic role for SJ proteins in the maintenance of salt and water balance in an aquatic insect. The present study provides insight into the contribution of the SJ protein Gli to the regulation of paracellular permeability properties in osmoregulatory epithelia of mosquito larvae in accord with altered environmental conditions such as salinity. Given the complexities of SJs as well as the many challenges of an aquatic lifestyle, our understanding of the important role of the SJs and their protein machinery in the physiology of larval mosquito homeostasis seems likely to grow with further investigations.

Acknowledgements

The authors would like to thank Dr Peter M. Piermarini at the Ohio State University for generously providing the anti-*Ae*AE antibody used in this study, and Dr Dennis Kolosov for his help with *in silico* analysis of the *A. aegypti* Gli sequence.

Competing interests

The authors declare no competing or financial interests.

Author contributions

Conceptualization: S.J., S.P.K., A.D.; Methodology: S.J., S.P.K., A.D.; Software: S.J.; Validation: S.J.; Formal analysis: S.J., S.P.K., A.D.; Investigation: S.J.; Data curation: S.J.; Writing - original draft: S.J.; Writing - review & editing: S.P.K., A.D.; Supervision: S.P.K., A.D.; Funding acquisition: S.P.K., A.D.

Funding

This study was funded by the Natural Sciences and Engineering Research Council of Canada (NSERC) Discovery Grants to S.P.K. and A.D., and an Ontario Graduate Scholarship to S.J.

Data availability

Aedes aegypti gliotactin sequence data have been submitted to GenBank under accession number KX823345.

References

Beyenbach, K. W., Skaer, H. and Dow, J. A. T. (2010). The developmental, molecular, and transport biology of Malpighian tubules. *Annu. Rev. Entomol.* **55**, 351-374.

Bradley, T. J. (1994). The role of physiological capacity, morphology, and phylogeny in determining habitat use in mosquitoes. In *Ecological Morphology* (ed. P. C. Wainwright and S. M. Reilly), pp. 303-318. Chicago, IL: The University of Chicago Press.

Byri, S., Misra, T., Syed, Z. A., Bätz, T., Shah, J., Boril, L., Glashauser, J., Aegerter-Wilmsen, T., Matzat, T., Moussian, B. et al. (2015). The triple-repeat protein anakonda controls epithelial tricellular junction formation in *Drosophila*. *Dev. Cell* **33**, 535-548.

Chasiotis, H., Ionescu, A., Misyura, L., Bui, P., Fazio, K., Wang, J., Patrick, M., Weihrauch, D. and Donini, A. (2016). An animal homolog of plant Mep/Amt transporters promotes ammonia excretion by the anal papillae of the disease vector mosquito *Aedes aegypti*. *J. Exp. Biol.* **219**, 1346-1355.

Clements, A. N. (1992). *The Biology of Mosquitoes*, Vol. 1. London: Chapman & Hall.

Del Duca, O., Nasirian, A., Galperin, V. and Donini, A. (2011). Pharmacological characterisation of apical Na^+ and Cl^- transport mechanisms of the anal papillae in the larval mosquito *Aedes aegypti*. *J. Exp. Biol.* **214**, 3992-3999.

Deligiannaki, M., Casper, A. L., Jung, C. and Gaul, U. (2015). Pasiflora proteins are novel core components of the septate junction. *Development* **142**, 3046-3057.

Donini, A. and O'Donnell, M. J. (2005). Analysis of Na^+, Cl^-, K^+, H^+ and NH_4^+ concentration gradients adjacent to the surface of anal papillae of the mosquito *Aedes aegypti*: application of self-referencing ion-selective microelectrodes. *J. Exp. Biol.* **208**, 603-610.

Donini, A., Patrick, M. L., Bijelic, G., Christensen, R. J., Ianowski, J. P., Rheault, M. R. and O'Donnell, M. J. (2006). Secretion of water and ions by Malpighian tubules of larval mosquitoes: effects of diuretic factors, second messengers, and salinity. *Physiol. Biochem. Zool.* **79**, 645-655.

Donini, A., Gaidhu, M. P., Strasberg, D. R. and O'Donnell, M. J. (2007). Changing salinity induces alterations in hemolymph ion concentrations and Na^+ and Cl^- transport kinetics of the anal papillae in the larval mosquito, *Aedes aegypti*. *J. Exp. Biol.* **210**, 983-992.

Edwards, H. A. (1982). *Aedes aegypti*: energetics of osmoregulation. *J. Exp. Biol.* **101**, 135-141.

Edwards, H. A. and Harrison, J. B. (1983). An osmoregulatory syncytium and associated cells in a freshwater mosquito. *Tissue Cell* **15**, 271-280.

Fiandra, L., Casartelli, M. and Giordana, B. (2006). The paracellular pathway in the lepidopteran larval midgut: modulation by intracellular mediators. *Comp. Biochem. Physiol. A Mol. Integr. Physiol.* **144**, 464-473.

Fournier, M. L., Paulson, A., Pavelka, N., Mosley, A. L., Gaudenz, K., Bradford, W. D., Glynn, E., Li, H., Sardiu, M. E., Fleharty, B. et al. (2010). Delayed correlation of mRNA and protein expression in rapamycin-treated cells and a role for Ggc1 in cellular sensitivity to rapamycin. *Mol. Cell Proteomics* **9**, 271-284.

Gilbert, M. M. and Auld, V. J. (2005). Evolution of clams (cholinesterase-like adhesion molecules): structure and function during development. *Front. Biosci.* **10**, 2177-2192.

Green, C. R. and Bergquist, P. R. (1982). Phylogentic relationships within the invertebrates in relation to the structure of septate junctions and the development of 'occluding' junctional types. *J. Cell Sci.* **53**, 279-305.

Günzel, D. and Yu, A. S. L. (2013). Claudins and the modulation of tight junction permeability. *Physiol. Rev.* **93**, 525-569.

Gupta, R., Jung, E. and Brunak, S. (2004). Prediction of N-glycosylation sites in human proteins. NetNGlyc 1.0 Server. http://www.cbs.dtu.dk/services/NetNGlyc/.

Halberg, K. A., Rainey, S. M., Veland, I. R., Neuert, H., Dornan, A. J., Klämbt, C., Davies, S.-A. and Dow, J. A. T. (2016). The cell adhesion molecule Fasciclin2 regulates brush border length and organization in *Drosophila* renal tubules. *Nat. Commun.* **7**, 11266.

Ichtchenko, K., Hata, Y., Nguyen, T., Ullrich, B., Missler, M., Moomaw, C. and Südhof, T. C. (1995). Neuroligin 1: a splice site-specific ligand for beta-neurexins. *Cell* **81**, 435-443.

Ichtchenko, K., Nguyen, T. and Sudhof, T. C. (1996). Structures, alternative splicing, and neurexin binding of multiple neuroligins. *J. Biol. Chem.* **271**, 2676-2682.

Izumi, Y. and Furuse, M. (2014). Molecular organization and function of invertebrate occluding junctions. *Semin. Cell Dev. Biol.* **36**, 186-193.

Izumi, Y., Yanagihashi, Y. and Furuse, M. (2012). A novel protein complex, Mesh-Ssk, is required for septate junction formation in the *Drosophila* midgut. *J. Cell Sci.* **125**, 4923-4933.

Izumi, Y., Motoishi, M., Furuse, K. and Furuse, M. (2016). A tetraspanin regulates septate junction formation in Drosophila midgut. *J. Cell Sci.* **129**, 1155-1164.

Jonusaite, S., Kelly, S. P. and Donini, A. (2013). Tissue-specific ionomotive enzyme activity and K^+ reabsorption reveal the rectum as an important ionoregulatory organ in larval *Chironomus riparius* exposed to varying salinity. *J. Exp. Biol.* **216**, 3637-3648.

Jonusaite, S., Donini, A. and Kelly, S. P. (2016a). Occluding junctions of invertebrate epithelia. *J. Comp. Physiol. B* **186**, 17-43.

Jonusaite, S., Kelly, S. P. and Donini, A. (2016b). The response of claudin-like transmembrane septate junction proteins to altered environmental ion levels in the larval mosquito *Aedes aegypti*. *J. Comp. Physiol. B* **186**, 589-602.

Jonusaite, S., Donini, A. and Kelly, S. P. (2017). Salinity alters snakeskin and mesh transcript abundance and permeability in midgut and Malpighian tubules of larval mosquito, *Aedes aegypti*. *Comp. Biochem. Phys. A* **205**, 58-67.

Kolosov, D. and Kelly, S. P. (2013). A role for tricellulin in the regulation of gill epithelium permeability. *Am. J. Physiol. Regul. Integr. Comp. Physiol.* **304**, R1139-R1148.

Linser, P. J., Neira Oviedo, M., Hirata, T., Seron, T. J., Smith, K. E., Piermarini, P. M. and Romero, M. F. (2012). Slc4-like anion transporters of the larval mosquito alimentary canal. *J. Insect Physiol.* **58**, 551-562.

Luquet, C., Pellerano, G. and Rosa, G. (1997). Salinity-induced changes in the fine structure of the gills of the semiterrestrial estuarian crab, *Uca uruguayensis* (Nobili, 1901) (Decapoda, Ocypodidae). *Tissue Cell* **29**, 495-501.

Luquet, C., Genovese, G., Rosa, G. and Pellerano, G. (2002). Ultrastructural changes in the gill epithelium of the crab *Chasmagnathus granulatus* (Decapoda: Grapsidae) in diluted and concentrated seawater. *Mar. Biol.* **141**, 753-760.

Nelson, K. S., Furuse, M. and Beitel, G. J. (2010). The *Drosophila* Claudin Kune-kune is required for septate junction organization and tracheal tube size control. *Genetics* **185**, 831-839.

Padash-Barmchi, M., Browne, K., Sturgeon, K., Jusiak, B. and Auld, V. J. (2010). Control of Gliotactin localization and levels by tyrosine phosphorylation and endocytosis is necessary for survival of polarized epithelia. *J. Cell Sci.* **123**, 4052-4062.

Padash-Barmchi, M., Charish, K., Que, J. and Auld, V. J. (2013). Gliotactin and Discs large are co-regulated to maintain epithelial integrity. *J. Cell Sci.* **126**, 1134-1143.

Patrick, M. L., Gonzalez, R. J., Wood, C. M., Wilson, R. W., Bradley, T. J. and Val, A. L. (2002). The characterization of ion regulation in Amazonian mosquito larvae: evidence of phenotypic plasticity, population-based disparity, and novel mechanisms of ion uptake. *Physiol. Biochem. Zool.* **75**, 223-236.

Patrick, M. L., Aimanova, K., Sanders, H. R. and Gill, S. S. (2006). P-type Na^+/K^+-ATPase and V-type H^+-ATPase expression patterns in the osmoregulatory organs of larval and adult mosquito *Aedes aegypti*. *J. Exp. Biol.* **209**, 4638-4651.

Piermarini, P. M., Grogan, L. F., Lau, K., Wang, L. and Beyenbach, K. W. (2010). A SLC4-like anion exchanger from renal tubules of the mosquito (*Aedes aegypti*): evidence for a novel role of stellate cells in diuretic fluid secretion. *Am. J. Physiol. Regul. Integr. Comp. Physiol.* **298**, R642-R660.

Rosenthal, R., Milatz, S., Krug, S. M., Oelrich, B., Schulzke, J.-D., Amasheh, S., Günzel, D. and Fromm, M. (2010). Claudin-2, a component of the tight junction, forms a paracellular water channel. *J. Cell Sci.* **123**, 1913-1921.

Schulte, J., Tepass, U. and Auld, V. J. (2003). Gliotactin, a novel marker of tricellular junctions, is necessary for septate junction development in *Drosophila*. *J. Cell Biol.* **161**, 991-1000.

Schulte, J., Charish, K., Que, J., Ravn, S., MacKinnon, C. and Auld, V. J. (2006). Gliotactin and Discs large form a protein complex at the tricellular junction of polarized epithelial cells in *Drosophila*. *J. Cell Sci.* **119**, 4391-4401.

Sharifkhodaei, Z., Padash-Barmchi, M., Gilbert, M. M., Samarasekera, G., Fulga, T. A., Van Vactor, D. and Auld, V. J. (2016). The *Drosophila* tricellular junction protein Gliotactin regulates its own mRNA levels through BMP-mediated induction of miR-184. *J. Cell Sci.* **129**, 1477-1489.

Smith, K. E., VanEkeris, L. A., Okech, B. A., Harvey, W. R. and Linser, P. J. (2008). Larval anopheline mosquito recta exhibit a dramatic change in localization patterns of ion transport proteins in response to shifting salinity: a comparison between anopheline and culicine larvae. *J. Exp. Biol.* **211**, 3067-3076.

Sohal, R. S. and Copeland, E. (1966). Ultrastructural variations in the anal papillae of *Aedes aegypti* (L.) at different environmental salinities. *J. Insect Physiol.* **12**, 429-434.

Venema, D. R., Zeev-Ben-Mordehai, T. and Auld, V. J. (2004). Transient apical polarization of Gliotactin and Coracle is required for parallel alignment of wing hairs in *Drosophila*. *Dev. Biol.* **275**, 301-314.

Yanagihashi, Y., Usui, T., Izumi, Y., Yonemura, S., Sumida, M., Tsukita, S., Uemura, T. and Furuse, M. (2012). Snakeskin, a membrane protein associated with smooth septate junctions, is required for intestinal barrier function in *Drosophila*. *J. Cell Sci.* **125**, 1980-1990.